

Microstructures and Magnetic Alignment of  $L1_0$  FePt Nanoparticles

G. B. Thompson – The University of Alabama  
et al.

Deposited 11/12/2018

Citation of published version:

Shishou, K., et al. (2007): Microstructures and Magnetic Alignment of  $L1_0$  FePt Nanoparticles. *Journal of Applied Physics*, 101(9). DOI: <https://doi.org/10.1063/1.2711803>

## Microstructures and magnetic alignment of $L1_0$ FePt nanoparticles

Shishou Kang,<sup>a)</sup> Shifan Shi, Zhiyong Jia, G. B. Thompson, David E. Nikles, and J. W. Harrell

*Center for Materials for Information Technology, The University of Alabama, Tuscaloosa, Alabama 35487-0209*

Daren Li, Narayan Poudyal, Vikas Nandwana, and J. Ping Liu  
*Department of Physics, University of Texas at Arlington, Arlington, Texas 76019*

(Presented on 11 January 2007; received 23 October 2006; accepted 14 December 2006; published online 9 May 2007)

Chemically ordered FePt nanoparticles were obtained by high temperature annealing a mixture of FePt particles with NaCl. After the NaCl was removed with de-ionized water, the transformed FePt nanoparticles were redispersed in cyclohexanone. X-ray diffraction patterns clearly show the  $L1_0$  phase. Scherrer analysis indicates that the average particle size is about 8 nm, which is close to the transmission electron microscopy (TEM) statistical results. The coercivity ranges from 16 kOe to more than 34 kOe from room temperature down to 10 K. High resolution TEM images reveal that most of the FePt particles were fully transformed into the  $L1_0$  phase, except for a small fraction of particles which were partially chemically ordered. Nano-energy dispersive spectroscopy measurements on the individual particles show that the composition of the fully transformed particles is close to 50/50, while the composition of the partially transformed particles is far from equiatomic. TEM images and electron diffraction patterns indicate  $c$ -axis alignment for a monolayer of  $L1_0$  FePt particles formed by drying a dilute dispersion on copper grids under a magnetic field. For thick samples dried under a magnetic field, the degree of easy axis alignment is not as high as predicted due to strong interactions between particles. © 2007 American Institute of Physics.

[DOI: [10.1063/1.2711803](https://doi.org/10.1063/1.2711803)]

### INTRODUCTION

Conventional magnetic recording media are quickly approaching the theoretical limit imposed by thermal fluctuations.<sup>1</sup> Following the seminal work of Sun and co-workers at IBM, much attention has been paid to self-assembled and monodispersed  $L1_0$  FePt and CoPt nanoparticles for future ultrahigh-density magnetic data storage media.<sup>2-7</sup> These nanoparticles are very small ( $<10$  nm), with uniform grain size and the ability to self-assemble into a regular array. The chemically ordered  $L1_0$  phase of the FePt system is of particular interest because of its high magnetocrystalline anisotropy energy density at the equiatomic composition that should allow the use of smaller, thermally stable magnetic grains and potentially lead to dramatic increases in storage density. Recently, Liu *et al.* have reported that the use of NaCl as a matrix can almost completely reduce the sintering of FePt nanoparticles during the  $L1_0$  phase transformation.<sup>8</sup> The fully transformed FePt particles show no grain growth and have large coercivity at room temperature. Another important issue for technological applications is how to align the magnetic easy axis of FePt nanoparticles. So far, only a small amount of work has been done on achieving magnetic alignment.<sup>9-11</sup> In this paper, we report a detailed study of the microstructure, magnetic properties, and easy axis alignment of  $L1_0$  FePt nanoparticles.

### EXPERIMENT

The synthesis of 8 nm FePt nanoparticles involves the thermal decomposition of  $\text{Fe}(\text{CO})_5$  and  $\text{Pt}(\text{acac})_2$  in an organic solvent using standard airless procedures as described in Ref. 12. The as-synthesized fcc FePt nanoparticles were mixed with ball-milled NaCl powder in hexane with the assistance of surfactants, oleic acid, and oleylamine as described in Ref. 8 for annealing.

The composition analysis of FePt nanoparticles determined by energy dispersive x-ray analysis on a Philips model XL 30 scanning electron microscope showed that there is negligible NaCl contamination in the salt-matrix annealed FePt nanoparticles, and the average atomic composition is about  $\text{Fe}_{52}\text{Pt}_{48}$ . Images of the magnetic particles were obtained on a Hitachi model H-8000 transmission electron microscope (TEM) and an FEI Tecnai F20 TEM. Bragg-Brentano x-ray diffraction (XRD) measurements ( $\theta$ -2 $\theta$  scans) were made on a Rigaku model D/MAX-2BX thin film diffractometer. Magnetic hysteresis curves were measured on an Oxford vibrating sample magnetometer (VSM) with temperature and magnetic field in the range of 5–300 K and 0–80 kOe, respectively.

### RESULTS AND DISCUSSION

The in-plane hysteresis loops shown in Fig. 1 exhibit large coercivity forces for the  $L1_0$  FePt nanoparticles.  $H_c$  increases from 16 kOe to more than 34 kOe with temperature measuring from room temperature down to 10 K. The actual  $H_c$  value at 10 K probably exceeds 34 kOe because

<sup>a)</sup>Electronic mail: skang@mint.ua.edu

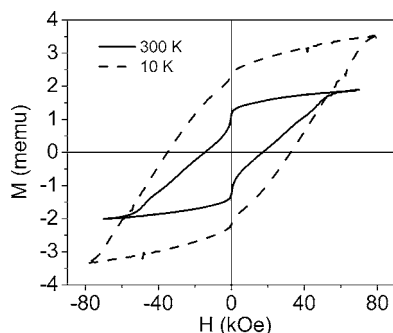


FIG. 1. The room and low temperature hysteresis loops of annealed FePt nanoparticles.

the maximum field on our VSM (80 kOe) was not sufficient to completely saturate the loop. The hysteresis loops also show a soft component in the  $L1_0$  FePt nanoparticles. Such a soft component might be related to partial chemical ordering of a small fraction the FePt nanoparticles, as will be discussed below.

Figure 2 shows a typical image of self-assembled  $L1_0$  FePt nanoparticles with average particle size around 8 nm, which is close to the grain size obtained from Scherrer analysis of XRD. The light and dark contrast shown in Fig. 2 is because of different crystallographic orientations of the FePt nanoparticles with respect to the beam normal incidence. The electron diffraction (ED) pattern clearly shows the  $L1_0$  phase and is consistent with the XRD measurements. From Fig. 2, it is clear that most annealed FePt nanoparticles exhibit single crystal structures with homogeneous contrast. However, there are a few FePt nanoparticles (for example, see the upper left corner FePt particle in Fig. 2) showing half light and half dark contrast. Thus, these nanoparticles are no longer single crystals after heat treatment for the  $L1_0$  phase transformation. In fact, these FePt nanoparticles are suspected to be partially chemically ordered.

The disordered A1 FePt phase has a fcc structure with  $a=0.3839$  nm and the  $L1_0$  FePt phase has a chemically ordered fct structure with  $a=0.3861$  nm and  $c=0.3788$  nm.<sup>13,14</sup> For FePt nanoparticles with a few nanometers in diameter, they prefer to form as a single crystal to minimize their total

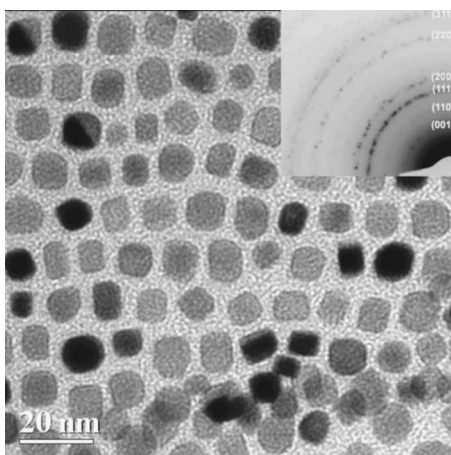


FIG. 2. TEM image of self-assembled FePt nanoparticles after annealing. Inset shows the ED patterns of these nanoparticles.

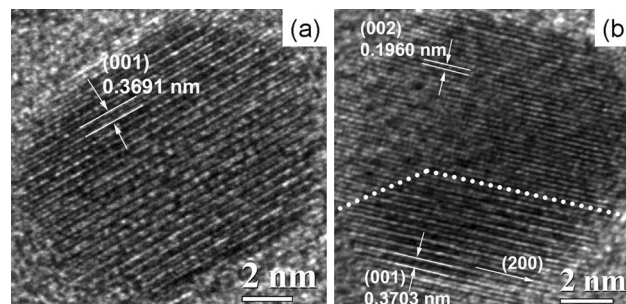


FIG. 3. HRTEM images of individual FePt nanoparticles after annealing: (a)  $\text{Fe}_{51}\text{Pt}_{49}$  and (b)  $\text{Fe}_{65}\text{Pt}_{35}$ . The composition was obtained with nano-EDS measurements.

energy. This was confirmed by the high resolution TEM (HRTEM) images for as-made FePt nanoparticles. However, as shown in Fig. 2, a few FePt nanoparticles after annealing show polycrystalline structures. Here HRTEM was applied to identify the microstructures of annealed FePt nanoparticles with single crystalline and polycrystalline phases. Figure 3(a) shows a HRTEM image of a  $\langle 100 \rangle$  oriented FePt nanoparticle that is fully phase transformed. The average measured interfringe distance for the  $\{001\}$  planes is 0.3691 nm, indicating the  $L1_0$  phase. Figure 3(b) shows the HRTEM images of FePt nanoparticles with multiorientations. The spacing of lattice fringes suggests partial chemical ordering in these FePt nanoparticles. Although the A1 (fcc) and  $L1_0$  (fct) FePt phases have very close lattice parameters, they can be distinguished by using the HRTEM image of  $\langle 001 \rangle$  oriented particles, because the  $[001]$  projected potential of  $L1_0$  FePt nanoparticles will have a composition modulation periodicity, whereas the A1 FePt nanoparticles do not.<sup>14</sup> If the top portion in Fig. 3 is a  $\langle 001 \rangle$  oriented grain with  $L1_0$  phase, there should exist composition modulation periodicity. This grain shows homogeneous contrast, indicating the fcc phase. Even if one is not directly on the zone axis, the periodicity of these lattice fringes should not change too noticeably.<sup>15</sup> The measured spacing does not match other interplanar spacings for the  $L1_0$  phase, i.e., different orientation in the nanoparticle for the  $L1_0$  phase, but has reasonably good agreement with the A1 phase. Nano-energy dispersive spectroscopy (EDS) analysis with a beam size  $\sim 4$  nm has shown that the most fully transformed FePt nanoparticles had an individual particle composition close to 50/50 stoichiometry [Fig. 3(a) caption]. However, for partially ordered FePt nanoparticles, it can either be Fe or Pt rich with composition far from equiatomic [Fig. 3(b)]. The compositions of these particles would place it beyond the bulk compositional phase field for the  $L1_0$  ordering.<sup>16</sup> This composition variation could inhibit the phase transformation and is the subject of further work. Although the total volume fraction of FePt nanoparticles with A1 phase is small, it will give a soft component to the  $M$ - $H$  curve as shown in Fig. 1 and result in a large switching field distribution (SFD).<sup>17</sup>

After the fct FePt nanoparticles were diluted with cyclohexanone in the presence of a small amount of vinyl chloride copolymer (MR104, a typical ligand for magnetic type particles),<sup>18</sup> the particles were dropped onto a carbon coated TEM grid under a 10 kOe magnetic field along the film

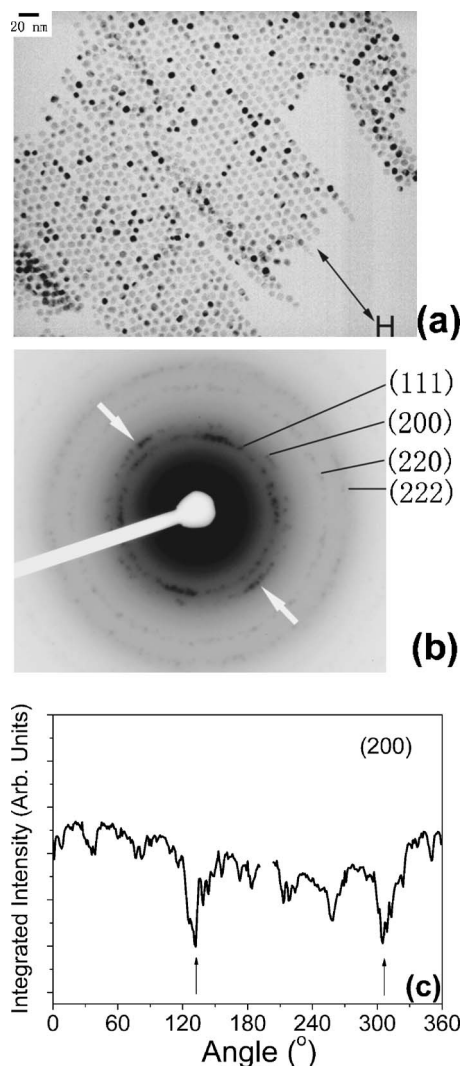


FIG. 4. (a) TEM image and (b) ED patterns of annealed FePt nanoparticles after aligning with 10 kOe in-plane magnetic field. (c) The angular dependence of integrated intensity of (200) diffraction ring shown in (b).

plane. Figures 4(a) and 4(b) show the respective TEM image and ED patterns of fct FePt nanoparticles after alignment. As can be seen in the image, the self-assembled fct FePt nanoparticles form chains along the magnetic field direction. The (001) diffraction ring is hard to discern because it is too close to the central direct beam. However, the (200) diffraction ring shows an intensity distribution that is much stronger along the aligning field direction [as indicated by the arrows in Fig. 4(b)]. We also plot the angular dependence of the integrated intensity of the (200) ring in Fig. 4(c). It clearly shows two strong peaks with twofold symmetry. Since it is hard to measure the magnetic properties of a sample on a TEM grid, we have tried to magnetically align a thick sample with a concentrated fct FePt nanoparticle dispersion under an in-plane magnetic field of  $\sim 5$  kOe. However, the degree of easy axis alignment is not as high as predicted by our previous model.<sup>11</sup> One possible reason might be because of the strong dipolar interactions between the fct FePt nanoparticles, which would make alignment difficult. Another possible reason might be because of the mobility of these fct

FePt nanoparticles under the large measuring field. For magnetic nanoparticles coated with organic surfactants, Klokkenburg *et al.* have found that these particles are still “free” to rotate under an external magnetic field even when the films are dried (due to the low glass transition temperature of the organic coatings).<sup>19</sup> Finding a possible way to fix the aligned FePt nanoparticles and achieve a high degree of alignment is the subject of future work.

In summary, we have studied the microstructural and magnetic properties of 8 nm FePt nanoparticles annealed with NaCl as a matrix. The XRD patterns, *M-H* loops, TEM images, and ED patterns clearly show the  $L1_0$  phase transformation of FePt nanoparticles with large coercivity without grain growth. Although most of FePt nanoparticles were fully transformed into the  $L1_0$  phase, HRTEM images reveal that there is a small fraction of FePt particles which were partially chemically ordered. Nano-EDS shows that the composition of the fully transformed particles is close to equiatomic, while the composition of partially transformed particles is far from equiatomic. We also demonstrated the *c*-axis alignment for monolayer  $L1_0$  FePt particles on a TEM grid. The intensity of (200) ED ring clearly show twofold symmetry.

#### ACKNOWLEDGMENTS

This work has been supported by the NSF Materials Research Science and Engineering Center Award No. DMR-0213985. J.P.L. acknowledges support by the U.S. DoD/MURI Grant No. N00014-05-1-0497 and DARPA through ARO under Grant No. DAAD 19-03-1-0038. The Technai TEM was acquired through NSF-MRI-0421376.

<sup>1</sup>D. Weller *et al.*, IEEE Trans. Magn. **36**, 10 (2000).

<sup>2</sup>S. Sun, C. B. Murray, D. Weller, L. Folks, and A. Moser, Science **287**, 1989 (2000).

<sup>3</sup>Z. R. Dai, S. Sun, and Z. L. Wang, Nano Lett. **1**, 443 (2001).

<sup>4</sup>S. Kang, J. W. Harrell, and D. E. Nikles, Nano Lett. **2**, 1033 (2002).

<sup>5</sup>X. Sun, Z. Jia, Y. Huang, J. W. Harrell, D. E. Nikles, K. Sun, and L. Wang, J. Appl. Phys. **95**, 6747 (2004).

<sup>6</sup>S. Kang, Z. Jia, D. E. Nikles, and J. W. Harrell, IEEE Trans. Magn. **39**, 2753 (2003).

<sup>7</sup>S. Sun, S. Anders, T. Thomson, J. E. E. Baglin, M. F. Toney, H. F. Hamann, C. B. Murray, and B. D. Terris, J. Phys. Chem. B **107**, 5419 (2003).

<sup>8</sup>J. P. Liu, K. Elkins, D. Li, V. Nandwana, and N. Poudyal, IEEE Trans. Magn. **42**, 3036 (2006).

<sup>9</sup>S. Yamamoto, Y. Morimoto, T. Ono, and M. Takano, Appl. Phys. Lett. **87**, 032503 (2005).

<sup>10</sup>S. Kang, Z. Jia, S. Shi, D. E. Nikles, and J. W. Harrell, Appl. Phys. Lett. **86**, 062503 (2005).

<sup>11</sup>J. W. Harrell, S. Kang, Z. Jia, D. E. Nikles, R. W. Chantrell, and A. Satoh, Appl. Phys. Lett. **87**, 202508 (2005).

<sup>12</sup>M. Chen, J. P. Liu, and S. Sun, J. Am. Chem. Soc. **126**, 8394 (2004).

<sup>13</sup>B. Stahl *et al.*, Phys. Rev. B **67**, 014422 (2003).

<sup>14</sup>J. Li, Z. L. Wang, H. Zeng, S. Sun, and J. P. Liu, Appl. Phys. Lett. **82**, 3743 (2003).

<sup>15</sup>D. B. Williams and C. B. Carter, *Transmission Electron Microscopy* (Plenum, New York, (1996).

<sup>16</sup>R. V. Chepulskaa and W. H. Butler, Phys. Rev. B **72**, 134205 (2005).

<sup>17</sup>S. Wang, S. S. Kang, J. W. Harrell, X. W. Wu, and R. W. Chantrell, Phys. Rev. B **68**, 104413 (2003).

<sup>18</sup>The MR104 used here was obtained from Nippon Zeon Corporation

<sup>19</sup>M. Klokkenburg, B. H. Erne, and A. P. Philipse, Langmuir **21**, 1187 (2005).